Volume: 02, Issue: 06, Pages:900-905 (2011)

Automated CAD for Nodule Detection for Magnetic Resonance Image Contrast Enhancement

K.R.Ananth
Assistant Professor, Department of MCA, Velalar College of Engineering and Technology, Erode, Tamil Nadu.
E-Mail : kmrananth@yahoo.com
Dr. S.Pannerselvam
Associate Professor of Computer Science, Erode Arts & Science College(Autono),Erode, Tamil Nadu.
E-Mail : pannirselvam08@gmail.com

----------ABSTRACT----------

Contrast is a measure of the variation in intensity or gray value in a specified region of an image. In all applications concerning image acquisition, followed by processing of images, successful pre-processing is of the essence. Every sensor has its own characteristics, but in general the quality of the acquired MR image is fairly poor. Overall grayscale intensity variations, poor contrast and noisy background are the frequently encountered issues. The Rational Unsharp Masking method is the one introduced here to improve the quality of the MR image. It is demonstrated, that the proposed method has much reduced noise sensitivity than another polynomial operator, Cubic Unsharp masking and number of approaches devised to improve the perceived quality of an image. This algorithm has been tested for various slices of axial, sagittal and coronal sections of MR image. The results confirm the ability of the algorithm to produce better quality images, helpful to have effective diagnosis.

Keyword - Image enhancement, Magnetic Resonance Image , Rational filters, Unsharp Masking.

Date of Submission: 15 October 2010 Date of Acceptance: 12 February 2011

1. INTRODUCTION

Digital cameras, new generation sensors and in general modern image acquisition devices, require algorithms for image enhancement suitable to work in real time and possibly with limited power consumption. Unfortunately most of the systems present in the literature either require a very high computational effort or do not provide good performances.

Image enhancement is discussed here as a processing technique to increase the visual contrast of an image in a designated intensity range or ranges. Although the degree of enhancement may be subjective, procedures to perform a given type of enhancement can be directly related to the most wanted purpose. Brain Images are often characterized not by particular objects, but by the global configuration of cerebrospinal fluid (CSF), gray matter (GM), white matter (WM) and white matter lesion (WML). The visual appearance of these images may be considerably improved by highlighting its high frequency contents to enhance the edge and detail information in it.

The spatial domain enhancement technique, histogram equalization improves contrast of the MR image by reassigning the brightness values of pixels based on the image histogram. Generally, images have unique brightness histograms. Even images of different areas of the same sample, in which the various structures present have consistent brightness levels wherever they occur, will have different histograms, depending on the area fraction of each structure. Here the pixel intensities are modified by a position invariant transformation function. The traditional histogram equalization method for MR image suffers from the following drawbacks:

(1) It lacks of a mechanism to adjust the degree of enhancement.

(2) It often causes unpleasant visual artifacts, such as over enhancement, level saturation and raised noise level.

(3) It could dramatically change the character of the image, e.g., the average luminance (mean) of the image. Changing the overall illumination of MR image will shifts the peaks in the histogram, there is a very little scope to improve contrast by global transformation.

As a result of the above shortcomings, histogram equalization is rarely used in its original form. In addition, most real images exhibit some variation in brightness within features (e.g., from the edge to the center) or in different regions.

In Unsharp Masking scheme, a scaled version of highpass filtered input signal is added to the signal itself to form the enhanced image. This enhances local features simply by removing or diminishing slowly varying attribute, thereby producing a constant background intensity distribution. Even though this method is simple

to implement, the presence of the linear highpass filter makes the system extremely sensitive to noise. This results in an undesirable distortion, particularly in uniform areas of the images. Furthermore, medium contrast details are not enhanced as like high contrast details in the image. Consequently to provide medium contrast detail areas with a good sharpening, the parameter of the linear unsharp masking algorithm must be set so as to emphasize the high contrast areas excessively. Therefore unpleasant overshoot artifacts appear in the output images.

To reduce the sensitivity to noise, modified Laplacian Sharpening is used, involves the convolution of an image with an operator known as the Laplacian. The Laplacian is a linear difference operator that is commonly used in the context of detecting edges that of course represent high frequency features in an image. The effect on an image of invoking the Laplacian is essentially equivalent to unsharp masking, subtracting a blurred version of the image from the original image. However, the Laplacian is very sensitive to noise and tends to amplify it; this limits its practical utility.

Homomorphic filtering for enhancement is a nonlinear operation that may be viewed as high-pass filtering not of image intensity rather of logarithm of image intensity. This technique details an image of a scene is assumed to be formed by the recording of the light reflected from an object that is illuminated by a source. Filtering with this method finds less practical importance because of dynamic range compression during transformation.

In this paper, we propose a Rational Unsharp Masking based enhancement scheme. The proposed method provides MR image sufficiently enhanced with a lesser amount of artifacts, and allows a convenient and effective control over the degree and effect of enhancement. In Section-3 of this paper, the cubic unsharp masking algorithm for 1D and 2D case is presented in detail for clear understanding of proposed method, while Section-4 describes the formulation of proposed rational operator which has been used. Results and comparisons are discussed in Section-4 followed by the conclusions in Section 6.

2. CUBIC UM OPERATOR

For the enhancement of the visual quality of an image, a Cubic Unsharp Masking (CUM) operator has been proposed. This operator belongs to the wide family of the polynomial operators, which have already been employed in various applications in the digital signal processing area. In the CUM technique the enhanced output is obtained by adding to the input signal a processed version of the signal itself, in which high frequency components are nonlinearly amplified. Referring for simplicity to the 1-D case, the output signal Y_n is obtained from the input X_n through the relation

$$Y_n = X_n + \lambda Z_n \quad (1)$$

where λ is a positive factor used to control the amount of correction. In turn, the correction term is expressed as

$$Z_n = (X_{n-1} - X_{n+1})^2 (2X_n - X_{n-1} - X_{n+1}) \quad (2)$$

This expression results from the product of a linear Laplacian filter and a modulation component $(X_{n-1} - X_{n+1})^2$; the latter is a quadratic function of an estimate of the local gradient, obtained through a bandpass filter [1]. Being quadratic, this function tends to privilege high-gradient areas and it is less sensitive to slow signal variations. Furthermore, the gradient estimate is performed using the bandpass filter $(X_{n-1} - X_{n+1})$; the response is good at medium frequency areas and decreases for higher frequencies. This makes the overall sharpening signal Z_n highly robust to noise than conventional linear Unsharp masking process and a choice for λ leads the dynamic range of the correction term for the cubic operator much larger than one specified for the linear UM filter. In order to reduce the overshoots in the output signal, this should in any case be truncated before displaying the data.

The general block diagram of UM method for 2-D signal is shown in fig.1

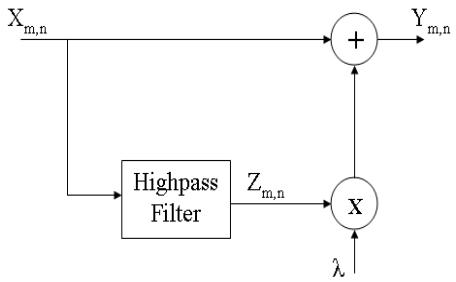

Fig.1 Basic Unsharp Masking Model

Here the correction signal $Z_{m,n}$ can be defined as

$$Z_{m,n} = [4 X_{m,n} - X_{m-1,n} - X_{m+1,n} - X_{m,n+1} - X_{m,n-1}] \quad (3)$$

Eq(4) is the simplest isotropic derivative operator which produces linear response, called Laplacian. Second order derivative have stronger response to fine details, such as thin lines, isolated points and double response to a gray-level step. More often Laplacian highlights gray-level discontinuities in an image and deemphasizes regions with slowly varying gray levels [2]&[3]. The first formulation of the 2-D CUM filter is deduced by adding the effects of the 1-D filter of Eq(2) applied in two orthogonal directions. If the horizontal and vertical directions are chosen, one obtains a "Separable Cubic UM filter"(S-CUM) expressed as

$$Z_{m,n} = (X_{m-1,n} - X_{m+1,n})^2 (2X_{m,n} - X_{m-1,n} - X_{m+1,n}) + (X_{m,n-1} - X_{m,n+1})^2 (2X_{m,n} - X_{m,n-1} - X_{m,n+1}) \quad (4)$$

A similar relation could be obtained by selecting the two diagonal directions. The second formulation of the CUM filter we put forward is "nonseparable Cubic UM filter" (NS-CUM) given as

$$Z_{m,n} = (X_{m-1,n} + X_{m+1,n} - X_{m,n-1} - X_{m,n+1})^2 (4X_{m,n} - X_{m-1,n} - X_{m+1,n} - X_{m,n+1} - X_{m,n-1}) \quad (5)$$

In Eq(4) & Eq(5), the same Laplacian filter as in Eq(3) is used with a modulation component, a quadratic function of an estimate of the local gradient. The response of S-CUM and NS-CUM along horizontal and vertical directions leads to square modulated values and null along diagonal directions. Usage of these filters with convenient choice of the coefficient λ will allows the luminance of the image pixels which are adjacent to the object border shall be either increased by some amount, if the pixel belongs to the object or decreased by the same amount if the pixel belongs to the background. Note that the coefficients of all filters sum to zero, indicates that they would give a response of zero in an area of constant gray level regions. The study which is presented in the following section will rectifies the drawbacks of such two filters, and it will give a basis for selecting rational filters according to the characteristics of the input MR image.

3. RATIONAL UM OPERATOR

A polynomial approach based on the basic UM scheme is still used here, but a *rational function (R^f)* (the ratio of two polynomials in the input variables) is introduced in the correction path. Employing such a function offers, details having low and medium sharpness are enhanced; on the other hand, noise intensification is very limited and steep edges, which do not need further emphasis, remain almost unaltered.

$$R^f = \left[\frac{\sum_{i,j \in W} R_{i,j} \cdot LF_{i,j}}{\sum_{i,j \in W} LF_{i,j}} \right] \quad (6)$$

The output Y(m,n) of the rational filter, as the input medical image X(m,n) is then computed in Eq(7)

$$Y(m,n) = X(m,n) + \lambda \{ Z_x(m,n)\, C_x(m,n) + Z_y(m,n)\, C_y(m,n) \} \quad (7)$$

where Z(m,n) is the correction term computed in both abscissa and ordinate as the output of a suitable enhancing filter, C(m,n) be the rational control term calculated along both horizontal and vertical direction and λ is a positive scaling factor. Rational operators given in Eq(8) be simple, designed in order to obtain the following effects:

1. To emphasize the details when these are poorly defined.
2. To limit the emphasis when the details are already very well defined in order to avoid the generation of annoying artifacts.
3. Finally, to reduce the signal when it is extremely weak, since in such case the information is superseded by the noise.

To this purpose, the two control signals be defined as

$$C_x(m,n) = \frac{G_x(m,n)}{k\, G^2_x(m,n) + h}, \quad C_y(m,n) = \frac{G_y(m,n)}{k\, G^2_y(m,n) + h} \quad (8)$$

where

$$G_x(m,n) = [X(m,n+1) - X(m,n-1)]^2$$
$$G_y(m,n) = [X(m+1,n) - X(m-1,n)]^2 \quad (9)$$

In Ref 2, relations are defined between the parameters ***k*** and ***h*** of the operator with respect to resonance peak at the abscissa G_0 given in Eq(9). Here the correction term Z(m,n) have been chosen to adapt the horizontal and vertical components separately since the human eye is known to be anisotropic in its sensitivity to the details along different orientations[4]. The filter which provides importance in edge preserving noise smoothing be given mathematically as

$$Z_x(m,n) = 2X(m,n) - X(m,n-1) - X(m,n+1)$$
$$Z_y(m,n) = 2X(m,n) - X(m+1,n) - X(m-1,n) \quad (10)$$

It is interesting to observe that once ***k*** and ***h*** of rational term is set, we can freely adjust the intensity of the enhancement using the parameter **λ.** It is apparent that the overall performance of the system can be satisfactory only if the activity measure G(m,n) is capable of representing important image features, without being mislead by noise. Furthermore, even very small details should be sensed by G(m,n) to achieve an effective sharpening action. The choice of correction and intensity control parameters are given in next section for various medical images with quality assessment.

4. NODULE DETECTION

The nodule detection is a very difficult step in every CAD system development. Actually, in MRI Brain images (Fig 2), nodules are frequently attached to blood vessels or to the pleura; and also the grey tone is so similar to vessel sections that traditional intensity-based methods are inappropriate. Instead, an effective nodule detection algorithm must take both the grey level and the object shape into account. In my CAD system we adopt a method that uses 3D shape information to identify spherical regions with a given grey level. The idea is to distinguish spherical from cylindrical (typically blood vessels) shapes analyzing a shape index (SI), defined in terms of 3D characteristics, extracted from sets of Voxels (Volumetric Picture Element) This Voxgram images are three-dimensional holograms that literally hang in space with grey level in the range of the nodule intensity.

The CAD system consists of CAD server and CAD workstation. The MRI data are transferred from the MRG scanner to the CAD server over the DICOM protocol [4]. The CAD server accepts and analyzes the scans by segmenting the lung parenchyma from the vessels, mediastinum, and chest wall. Other techniques are used to include lesions that may be touching the chest wall. The CAD workstation is user controlled. The findings of CAD are presented in three windows on the monitor the original 3D axial images and a brain nodule map.

The suspected lesions are circled on the nodule map. When these circled nodules are clicked with the mouse, the appropriate axial slice will appear, with the suspected nodule encircled. Also, the appropriate region on the 3D window appears with the suspected nodule colored. The 3D image can be rotated and otherwise modified for the radiologist to decide if it is a true nodule or not. The size, volume, and density of the nodule are displayed on the left. A nodule can also be added by the radiologist and it will be surrounded by a hexagon. The size, volume, and density are also determined by the CAD system.

Functional Magnetic Resonance Imaging (fMRI) is the dominant method for non-invasive dynamical analysis of brain function. It involves the use of Magnetic Resonance (MR) scanner to rapidly obtain images of brain state. fMRI allows the researcher to observe brain activity of a subject for example while it is performing some task and therefore better understand brain organization and function. fMRI depends on the ability of MR scanners to detect regional changes in oxygenation level of the blood following neural activity [5]. That is, it indirectly observes brain activity on the neuronal level. The blood oxygen level dependency (BOLD) response to stimulus is often modelled as a hump like function that reaches maximum in about 5 seconds and dies out after about 10 seconds [6]. In practice it is usually assumed that the BOLD response is linearly related to the stimulus; [7] shows that this assumption is correct to the first order.

In a typical experiment an MRI scanner is used to record signals that can be used to construct a sequence of brain activation images with a typical sampling time 2-5 sec while the subject reacts to a stimulus, e.g., auditory, visual, motor, etc. A typical blocked experiment usually consists of two states; the control state and a functional state. The functional state could for example involve finger tapping or a visual fixation on a flickering image and the rest state involves no motor action or visual fixation on non-flickering image.

5. RESULTS AND DISCUSSIONS

We have tested our methods on various types of images. In this section, we have taken several examples of medical images and demonstrate the enhanced results. Unlike many other medical imaging models, the contrast in an MR image by acquisition depends strongly upon the way the image is acquired. By altering RF and gradient pulses, and by carefully choosing relaxation timings, it is possible to highlight different components in the object being imaged and produce high contrast images. Test has been made on both normal and abnormal images acquired on a 0.2 Tesla, Siemens – magnetom CONCERTO MR Scanner (Siemens, AG Medical Solutions, Erlangen, Germany) from Janson's MRI and CT scans Erode, INDIA. The scan image was taken with sagittal, Coronal, axial , 2Dand 3D, 2mm thick slice, with a slice gap of 2mm, with 246*512 acquisition matrix and with the field view of 250mm.

Fig.2(a) shows a brain MR image with low contrast. The enhanced image after applying histogram equalization (HE), the result by Cubic Unsharp Masking (with λ = 0.001) and Rational Unsharp masking (with λ = 0.00125) are shown in Fig.2(b) to (d) respectively. Histogram equalization (HE) as shown in Fig.2(b), makes a considerable change in intensity distribution of MRI image which causes unpleasant visual artifacts and dramatically change the average luminance (mean) of the image. It also hides some important line-shaped structures in high intensity background which is most wanted for clear diagnosis.

A performance evaluation of different transformation algorithms is inherently difficult to obtain, due to the lack of appropriate measures for judging the quality of the image resulting from the enhancement process. None of the quality measures suggested in the literature has achieved widespread acceptance as a universal measure, since the evaluation of the quality of the enhanced image is subjective, in that it depends on display devices, observers and viewing conditions.

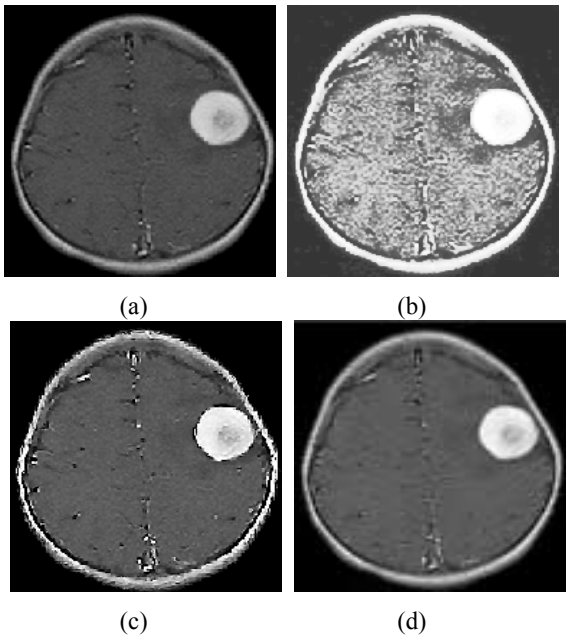

Fig.2 (a)Brain MRI Axial Slice (b) Histogram Equalized Image (c) Result of CUM (d) Result of Rational UM

The most reliable quality criterion is the visual appearance; however, here an objective measure named correlation co-efficient is used to judge the quality of the response. Though histogram equalization is powerful in highlighting the borders and edges between different objects, but may reduce the local details within these objects, especially smooth and small ones. Fig.2(c) shows the enhanced image obtained by applying CUM operator.

At this juncture CUM results in an undesirable distortion particularly in the areas of edges. Rational unsharp Masking Technique on Brain MRI offers more enhancements on Low contrast details, Medium contrast details are moderately enhanced and high contrast pixels are unchanged. Noise amplification is very limited and steep edges are not further emphasized.

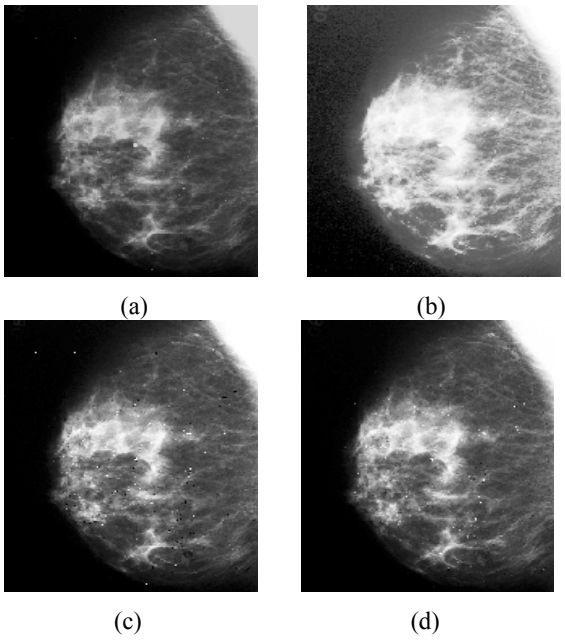

(a) (b)

(c) (d)

Fig.3 (a) Mammogram image (b) Histogram Equalized Image (c) Result of CUM (d) Result of Rational UM

Fig.3(a) shows mammogram image; it's enhanced version using the proposed technique shown in Fig.3(c). The best visual quality is obtained for mammogram when k=0.00125, h=200 and λ = 1.2. Image by Rational UM method clearly shows the nodules and dense masses present in the mammogram without incur significant noise amplification, where CUM introduces artifacts in background and details regions. Since sharpening signal in CUM is highly robust to noise, provisions are available to judge benign findings as malignant masses. Besides images shown in Fig.3, correlation co-efficient value for mammogram in Table.1 also quantifies our proposed technique as prominent.

An X-ray image of pelvic region is also taken as a sample image for testing. Fig. 4 shows the uterine cavity and fallopian tubes that are opacified by injecting a contrast (iodine) into the uterus through a catheter, which looks white on the image. Enhancement through histogram equalization produces improved contrast for all levels of intensities in the original image. Effect of CUM on

Table 1: Correlation Co-efficient of Processed Images through Various Filters

Filter	Brain MRI Axial Slice	Breast Image	Uterus X-ray image	Flower Image
HE	11.7081	8.4673	17.9044	38.1781
Linear UM	9.0443	6.3079	14.0378	15.0346
Cubic UM	4.7742	5.5460	12.3169	2.9460
Rational UM	**8.8005**	**6.0742**	**16.9308**	**31.2397**

Fig.4(a) leads overshoots in the areas of sharp transitions. The evaluation results given in Table-1 also least than proposed method and HE.

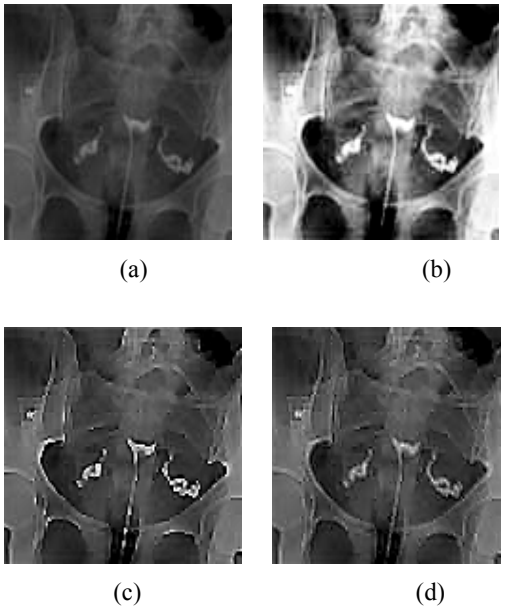

(a) (b)

(c) (d)

Fig.4 (a) Uterus X-ray Image (b) HE Image (c)Result of CUM (d) Result of Rational UM

Fig.3 (a) Sample Flower Image(b) Histogram Equalized Image (c) Result of CUM (d) Result of Rational UM

6. CONCLUSION

In this paper, the purpose in developing an automatic CAD system for early detection of Brain, Brest and Kidney cancer can be analyzed with raw organ MRI images is achieved after performing many experiments. The approach starts by extracting the lung regions from the MRI image using several image processing techniques, including bit plane slicing, erosion, median filter, dilation, outlining, and flood-fill algorithm. The author introduced the using of bit-plane slicing technique instead of the thresholding technique that is used in the first step in the extraction process to convert the MRI image into a binary image. Bit-plane slicing technique is both faster and data- and user-independent compared to the thresholding technique. After the extraction step, the extracted Brain regions are segmented using fuzzy possibility of c mean (FPCM) algorithm. The HANN algorithm shows homogeneous results obtained in a short time. Then, the initial lung candidate nodules resulting from the HANN segmentation are analyzed to extract a set of features to be used in the diagnostic rules. These rules are formulated in the next step to discriminate between cancerous and non-cancerous candidate nodules.

The advantages of the FPCM method are the following: (1) it yields regions more homogeneous than those of other methods, (2) it reduces the spurious blobs, (3) it removes noisy spots, and (4) it is less sensitive to noise than other techniques. This technique is a powerful method for noisy image segmentation and works for both single and multiple-feature data with spatial information. The extracted features in the proposed system are: the segmented lung regions, the maximum drawable circle (MDC) inside the region and the mean pixel intensity value of the region.

The results achieved by the author are: On one hand, the author have developed an automatic CAD system for early detection of lung cancer using chest CT images in which a high level of sensitivity has been achieved, with a reasonable amount of false positives per image, (90% sensitivity with 0.05 false positives per image). This prevents the system from hindering the radiologist's diagnosis. On the other hand, the proposed CAD system is capable of detecting lung nodules with diameter $\geq$ 2 mm, which means that the system is capable of detecting lung nodules when they are in their initial stages. Thus facilitating early diagnosis will improve the patients' survival rate.

7. REFERENCES

[1] Singapore Cancer Society, "http://www.singaporecancersociety.org.sg".

[2] American Cancer Society, "Cancer Statistics, 2005", CA: A Cancer Journal for Clinicians, 55: 10-30,2005,

[3] R. Wiemker, P. Rogalla, T. Blaffert, D. Sifri, O. Hay, Y. Srinivas and R. Truyen "Computer-aided detection (CAD) and volumetry of pulmonary nodules on high-resolution CT data", (2003).

[4] K. Kanazawa, Y. Kawata, N. Niki, H. Satoh, H. Ohmatsu, R. Kakinuma, M. Kaneko, N. Moriyama and K. Eguchi, "Computer-aided diagnosis for pulmonary nodules based on helical CT images", Compute. Med. Image Graph, vol. 22, no. 2 (1998), pp. 157-167.

[5] S. Ogawa, D.W. Tank, R. Menon, J.M. Ellerman, S.G. Kim, and H. Merkle. Intrinsic signal changes accompanying sensory stimulation: Functional brain mapping with magnetic resonance imaging. Proc. Natl. Acad. Sci. USA, 89:5951–5955,1992.

[6] R.B. Buxton. Introduction to Functional Magnetic Resonance Imaging: Principles and Techniques. Cambridge University Press, Cambridge, England, 2002.

[7]. G.M. Boynton, S.A. Engel, G.G. Glover, and D.J. Heeger. Linear Systems Analysis of Functional Magnetic Resonance Imaging in Human V1. The Journal of Neuroscience, 16(13):4207–4221, 1996.

[8]. K.J. Friston, P. Jezzard, and R. Turner. Analysis of functional MRI series. Human Brain Mapping, pages 153–171, 1994.

[9]. M.J. McKeown, S. Makeig, Brown G.G., Jung, Bell A.J. Kinderman, S.S., and T.J. Sejnowski. Analysis of fMRI data by blind separation into independent spatial component. HumanBrain Mapping.

[10]. M. Feilner, T. Blu, and M. Unser, "Statistical analysis of fMRI data using orthogonal filterbanks," in Proc. of SPIE Conference onWavelet Applications in Signal and Image Processing, 1999, pp. 551–560.